

## Aggregation of algae released from melting sea ice: implications for seeding and sedimentation\*

U. Riebesell<sup>1</sup>, I. Schloss<sup>2</sup> and V. Smetacek<sup>1</sup>

<sup>1</sup> Alfred-Wegener-Institut für Polar- und Meeresforschung, Columbusstrasse, W-2850 Bremerhaven, Federal Republic of Germany

<sup>2</sup> Instituto Antártico Argentino, Cerrito 1248, (1010) Buenos Aires, Argentina and CONICET, Argentina

Received 5 November 1990; accepted 20 January 1991

**Summary.** Factors influencing the fate of ice algae released from melting sea ice were studied during a *R/V Polarstern* cruise (EPOS Leg 2) to the northwestern Weddell Sea. The large-scale phytoplankton distribution patterns across the receding ice edge and small-scale profiling of the water column adjacent to melting ice floes indicated marked patchiness on both scales. The contribution of typical ice algae to the phytoplankton was not significant. In experiments simulating the conditions during sea ice melting, ice algae revealed a strong propensity to form aggregates. Differences in the aggregation potential were found for algal assemblages collected from the ice interior and the infiltration layer. Although all algal species collected from the ice were also found in aggregates, the species composition of dispersed and aggregated algae differed significantly. Aggregates were of a characteristic structure consisting of monospecific microaggregates which are likely to have formed in the minute brine pockets and channels within the ice. Sinking rates of aggregates were three orders of magnitude higher than those of dispersed ice algae. These observations, combined with the negligible seeding effect of ice algae found during this study, suggest that ice algae released from the melting sea ice are subject to rapid sedimentation. High grazing pressure at the ice edge of the investigation area is another factor eliminating ice algae released during melting.

### Introduction

The sea ice girdle around Antarctica harbours a rich assemblage of organisms that can attain high biomass concentrations in spring, prior to melting of this transient habitat (Ackley et al. 1979; Palmisano and Sullivan 1983; Garrison and Buck 1989). It has been increasingly realized during the past decade that algae present in or on sea ice play an important role in the ecology of polar waters. One

of the functions attributed to these organisms is that of a seed stock released to the water column during ice melt (Garrison and Buck 1985; Smith and Nelson 1985; Garrison et al. 1987). The supply of viable cells to the melt water lenses that arise adjacent to retreating ice edges is an important factor determining the growth rate of phytoplankton blooms that develop under such conditions. As melt-water lenses are favourable but transient environments for algal growth, the biomass attained within such a melt water layer (disregarding losses) is a product of the original seed stock multiplied by the cell division rate. Thus, input of cells from ice to the water column may be an important parameter for assessing the productivity of polar waters.

Ice algae released to the water during melting either continue growth in the surface layer or are subject to elimination by sinking to greater depths (Sasaki and Hoshiai 1986; Carey 1987) or grazing by pelagic herbivores (O'Brien 1987; Marschall 1988; Daly and Macaulay 1988). As sinking of unicellular algae is greatly enhanced by aggregate formation (Alldredge and Silver 1988), the propensity to form aggregates hence determines whether a given algal assemblage will remain in suspension or tend to sink out of the surface layer.

A tool to estimate the potential for aggregate formation—the roller table—has been recently developed by Shanks and Edmondson (1989). This technique involves rotating a transparent cylinder containing the sample for a period of several hours. By this means, particles are maintained in suspension. A few minutes after the beginning of rotation, the enclosed body of water has reached the same speed of rotation as the tank walls. Given that the tank was filled without air bubbles, the system will be free of shear motion and differential settling becomes the dominant mechanism bringing particles of different size and density into contact (Jackson 1990). Physical aggregation will occur only if particle surfaces are sticky. In this case, aggregation continues until all potentially sticky particles are incorporated. In the absence of stickiness, particles will remain dispersed. The time elapsing until the first aggregates appear and the period until

\* Data presented here were collected during the European *Polarstern* Study (EPOS) sponsored by the European Science Foundation

their growth stops are measures of the aggregation potential of the particles in the sample. Aggregates formed by this technique have been shown to closely resemble those occurring in nature (Shanks and Edmondson 1989) and have the advantage of being readily available for further analyses. In this study we employed the roller table to assess the aggregation potential of ice algae.

The present study was part of the interdisciplinary investigation of the seasonal development of sea ice and water column biota carried out in the framework of the European Polarstern Study (EPOS). This series of cruises was centered on the ice edge of the northwestern Weddell Sea. The expeditions provided a unique opportunity to study, over a prolonged period, the fate of ice algae released from melting ice and to assess their role in seeding phytoplankton populations developing in melt water layers. Growth potential in relation to light intensity of ice and water column algae was studied by Mathot et al. (in press); grazing experiments with krill and copepods on algae from both habitats were carried out by Riebesell et al. (in preparation). In this paper, we compare distribution patterns of phytoplankton and ice algal species composition on both regional scales across the receding ice edge, and local scales in the close vicinity of melting ice floes. Aggregation potential and sinking rates of aggregates and dispersed algae were measured in order to assess the possible role of sinking in eliminating ice algae from the mixed layer.

## Materials and methods

### Field sampling

The investigation presented herein was conducted during EPOS Leg 2 across the Weddell Scotia Confluence from November 19th, 1988 to January 9th, 1989. A total of 4N/S transects along 49° W and 47° W were carried out across the ice edge from open water at 57° S to deep within the closed pack at approx. 62° S (Fig. 1). Ice coverage was monitored during these transects (Franeker 1989). Water column stations were carried out at 30 nautical miles (nm) intervals. A variety of parameters pertaining to hydrography, chemistry and biology were measured at these stations (Hempel et al. 1989). No systematic survey of the distribution of ice properties was carried out, however ice cores were taken on 4 occasions throughout the cruise from ice floes selected on the basis of their colouration. These samples were utilized for physiological studies of the ice algae.

In order to assess small-scale distribution of phytoplankton adjacent to the ice edge, a survey was conducted from the 7th to 8th of December. Bucket samples were collected at 2.5 nm intervals along two parallel transects between 58° 55'S and 59° 30'S. These transects were ca. 10 nm apart and positioned roughly diagonal to the ice edge. The chlorophyll *a* content of these samples was analysed and the dominant phytoplankton species identified.

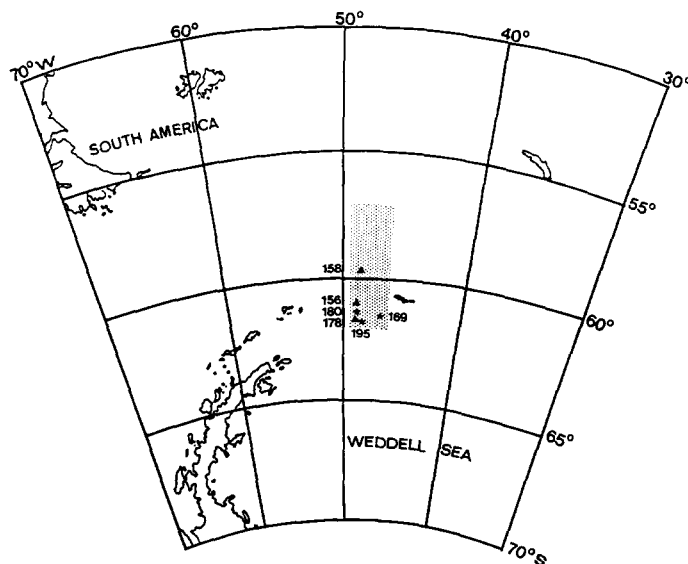


Fig. 1. Map showing study area of the expedition EPOS Leg 2 and locations of stations for small-scale profiling of the water column adjacent to coloured ice floes (Stations 156, 158, 178; triangles) and for sea ice sampling (Stations 169, 180, and 195; asterisks)

At Stations 156, 158, and 178 (Fig. 1), small-scale sampling of the water between melting ice floes was carried out from a rubber dinghy and from the edges of floes in order to assess horizontal and vertical distribution of ice algae freshly released from the ice. At a total of nine sites, the water and ice surface were closely examined for the presence of attached or floating algal aggregates and also for krill. Discrete samples were pumped through a tube from the surface to a 1 m depth. Three to four samples were collected per profile. The edges of greenish-brown coloured (i.e. algal-containing) melting ice floes, brash ice fields and the open water in between these ice floes were sampled. Salinity and chlorophyll concentrations were determined on these samples.

At three stations different kinds of sea ice were sampled (Table 1). At Stat. 169, small pieces of ice were cut off from the outer edge of an ice floe just below the water level. This floe had a distinctly brown colouration that extended to well below the water level. At Stat. 180, a ca. 1 m<sup>3</sup> block of brown ice broken off by *Polarstern* from an intact floe was heaved on board. Subsamples were taken from the inner part of the ice block. At Stat. 195, pieces of ice from the infiltration layer, i.e. the algal enriched layer at the snow-ice interface, were sampled after removal of the snow layer above water level.

### Laboratory experiments

After collecting the ice samples, small algal aggregates attached to the ice surface were removed and examined under the microscope. These will be referred to as natural aggregates below. The ice was placed in an equal volume of GF/F-filtered seawater for osmotically buffered melting (Garrison and Buck 1986) at 0°C for 10 to 12 h. The

Table 1. Sea ice samples collected for aggregation experiments

Stat. no.	Date	Location	Ice cover	Sample
169	16/12/1988	61°30.3'S 47°00.1'W	85%	ice interior assembl.
180	25/12/1988	61°25.7'S 49°01.8'W	30%	ice interior assembl.
195	31/12/1988	61°45.7'S 48°43.4'W	90%	infiltr. layer assembl.

ice was removed before complete melting and the algal enriched water was mixed and transferred into 3 replicate 10 l cylindrical plexiglass tanks under air exclusion. Subsamples were taken for light-microscopic analyses, as well as the determination of salinity, chlorophyll *a*, and phaeopigment concentrations. The plexiglass tanks were then rotated at 7 revolutions per minute as described by Shanks and Edmondson (1989). Temperature and illumination were maintained at 0°C and  $60 \mu\text{E m}^{-2} \text{s}^{-1}$  with a light/dark cycle of 16/8 h respectively. This treatment was used to examine the potential for aggregate formation under conditions expected to occur in melt water lenses prevailing during the release of ice algae into the open water.

Upon the start of rotation, one of the three tanks from each station was photographed at 10 min intervals. With increasing time of rotation, ranging to periods of 10–12 h, the photographing frequency was gradually decreased to 60 min intervals. The photographs were enlarged to 3 times the natural size and analysed for number and size of aggregates  $>0.5 \text{ mm}^2$  projected area. Aggregation potential was determined from the increase in aggregate size and abundance over time. The period of rotation was terminated after 24 h (Stat. 169), 10 h (Stat. 180, first tank), 22 h (Stat. 180, second and third tanks), and 30 h (Stat. 195). The tanks were then opened, aggregates collected by pipette, and the surrounding water sampled by syringe. Subsamples of both were fixed with formalin (2% final concentration) for light microscopic analysis of the algal species composition and SEM examination of the aggregate structure.

For determination of aggregate sinking rate, individual aggregates were carefully siphoned from the tanks into glass pipettes (10 mm in diameter). After measuring their diameter, intact aggregates were placed in a 110 cm long, 10 cm wide plexiglass tube filled with GF/F-filtered seawater. The time of sinking was measured at 5 cm intervals. The sinking rate was calculated from measurements in which the rate remained constant over several measuring intervals. Since both aggregation in the rotating tanks and aggregate handling during transfer from the tanks to the settling column may have artificially compacted the aggregates, lab measurements are likely to overestimate *in situ* aggregate sinking rates (cf. Shanks and Trent 1980; Alldredge and Gotschalk 1988). The sinking rate of the non-aggregated phytoplankton was determined using the SETCOL homogeneous sample method (Bienfang 1981). After measuring the initial chlorophyll *a* concentration, two replicate 1.2 l samples of surrounding water were filled into 50 cm long settling columns. After a settling period of 4 h, the upper and lower 100 ml were sampled and chlorophyll *a* concentrations measured. Sinking rates were calculated according to the equations outlined by Bienfang (1981).

### Analytical techniques

The salinity was measured with a Guildline Autosol Salinometer. For the determination of chlorophyll *a*- and phaeopigment concentrations, samples were filtered onto 25 mm Whatman GF/C glass fiber filters. After extraction in 90% acetone (filters were homogenized with glass beads in a cell mill), the samples were analysed using standard fluorometric methods (Parsons et al. 1984). Light microscopic analyses of both water samples and intact ice algal aggregates were carried out using the inverted microscope method of Utermöhl (1958). In the case where aggregates were too dense to be analysed in their existing form, they were gently squeezed between slide and cover-slip and examined under a standard microscope. For scanning electron microscopy (SEM), individual aggregates were dehydrated through an alcohol series, critical-point-dried in liquid  $\text{CO}_2$ , and platinum-palladium coated immediately after dehydration. Aggregates were then examined on an ISI D 130 SEM.

Oxygen production and consumption was measured by incubating aggregated and non-aggregated algae at a light intensity of  $95 \mu\text{E m}^{-2} \text{s}^{-1}$  and in the dark. Non-aggregated algae, individual aggregates placed in filtered seawater, and controls with filtered seawater only were incubated in 20 ml glass vials for 16 h at a temperature of 0°C. The oxygen concentration in the water was

measured with a Radiometer Acid-Base Analyzer equipped with an E-5046 electrode before and after incubation. The chlorophyll *a* concentrations of the incubated samples were determined and the rate of oxygen production/consumption expressed per unit chlorophyll *a* ( $\text{ml O}_2 \text{ mg Chl. a}^{-1} \text{ h}^{-1}$ ).

## Results

### Visual observations from ship-deck

The distribution of algal-rich ice floes of strong brown or yellow colouration that contrasted strikingly with the white of barren ice floes was highly patchy throughout the investigation period. Fields of rich brown ice floes ranging from tens of meters up to several kilometres in extent were recorded from the beginning of the study and also during the preceding *Polarstern* cruise (EPOS Leg 1) to the same area in October/November (Hempel 1989). On the other hand, extensive fields of large, white ice floes dominated the ice cover encountered just south of the ice edge at 61°S as late as early January. Thus, although no systematic records of the degree of brown colouration of the ice cover were made, the general impression we gained was one of great spatial variability not subject to a distinct seasonal trend during the period of observation (mid-October through early January).

### Water column properties of the marginal ice zone

The chlorophyll *a* distribution at different space and time scales at the melting ice edge is given in Tables 2 and 3 and Fig. 2. Values recorded during the transects are presented in relation to percentage ice cover in Table 2. Values under denser ice cover were consistently lower than those some distance from the ice edge. The maximum chlorophyll *a* values recorded along each transect were measured approximately 60–90 nautical miles north of the respective ice edge. An interesting feature of these maxima was that different species dominated the crop in each case (various centric diatoms along transects 1 and 2, cryptophycean and unidentified nanoflagellates along transects 3 and 4) and that typical ice algae did not contribute substantially to the phytoplankton biomass in any of the cases.

The results of the small-scale survey of the ice edge assemblage depicted in Fig. 2 indicate great spatial variation both in biomass and in the dominant species composition. The patch of higher chlorophyll *a* values in the area covered by dispersed ice floes could be attributed primarily to one or several species of the flagellate genus *Cryptomonas*, which was not recorded within the ice itself. In some cases, the ice algae *Nitzschia* spp. played a secondary role. To the north away from the ice (sampling sites no. 5–7), characteristic pelagic diatom species dominated. With the occasional exception of *Nitzschia* spp., the typical ice algae only contributed negligibly to water column assemblages throughout this survey.

Small-scale profiles of salinity and chlorophyll *a* (Table 3) were recorded around melting ice floes deep within the ice cover (Stats. 156 and 178) and at the outer

**Table 2.** Chlorophyll *a* concentration (mg Chl. *a* m<sup>-3</sup>) at 10 m water depth at selected stations during four N-S transects along the 49°W (1st, 3rd, and 4th transect) and the 47°W (2nd transect) meridian in relation to ice cover

Ice cover	Transect			
	1st	2nd	3rd	4th
	27 Nov.–12 Dec.	13 Dec. 16 Dec.	20 Dec.–26 Dec.	27 Dec.–4 Jan.
0% <sup>a</sup>	0.16 (57°29.9'S)	0.15 (57°59.5'S)	0.85 (57°29.9'S)	0.88 (58°59.9'S)
0% <sup>b</sup>	3.83 (58°30.0'S)	1.07 (59°29.9'S)	2.41 (59°29.7'S)	3.64 (60°30.0'S)
20%–40%	1.32 (59°59.5'S)	0.52 (60°30.2'S)	1.12 (60°58.3'S)	0.52 (61°31.1'S)
>80%	0.20 (61°59.5'S)	0.62 (61°30.3'S)	0.47 (61°28.8'S)	0.28 (61°44.7'S)

<sup>a</sup> Stations 2° (120 nautical miles) north of first ice

<sup>b</sup> Highest chlorophyll *a* value during transect, in all transects this station was located 60–90 nautical miles north of first ice

**Table 3.** Vertical profiles of salinity (‰) and chlorophyll *a* concentration (mg Chl. *a* m<sup>-3</sup>) taken along the 49° W meridian at 9 sites in the close vicinity of melting colourized ice floes on 3/4 Dec. (Stat. 156, 50% ice cover), 9 Dec. (Stat. 158, 5% ice cover), and 23 Dec. (Stat. 178, 90% ice cover)

Station 156 (60°59.8'S)										
Depth (m)	A		B		C		D		E	
	Sal.	Chl. <i>a</i>	Sal.	Chl. <i>a</i>	Sal.	Chl. <i>a</i>	Sal.	Chl. <i>a</i>	Sal.	Chl. <i>a</i>
0	33.06	1.15	33.70	0.68	33.99	0.41	33.98	0.69	33.42	0.48
0.13	–	–	–	–	33.99	0.44	34.03	0.49	34.02	0.50
0.25	33.97	0.54	33.96	0.53	34.01	0.43	34.03	0.49	34.02	0.50
0.50	34.03	0.55	34.01	0.54	34.05	0.46	34.05	0.48	34.04	0.49
20	34.05	0.51	34.05	0.51	34.11	0.34	34.11	0.34	34.11	0.34

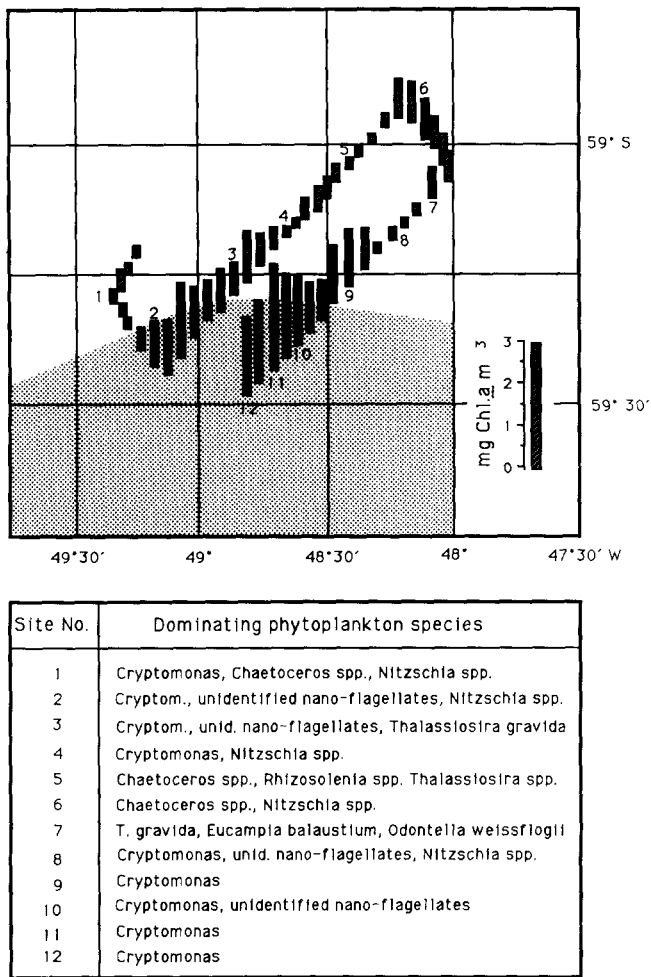
  

Station 158 (59°27.7'S)					Station 178 (61°28.8'S)			
Depth (m)	A		B		A		B	
	Sal.	Chl. <i>a</i>	Sal.	Chl. <i>a</i>	Sal.	Chl. <i>a</i>	Sal.	Chl. <i>a</i>
0	33.19	1.68	32.99	1.46	29.77	0.61	32.91	0.66
0.25	33.27	1.95	33.17	1.58	33.68	0.48	33.80	0.46
0.50	–	–	–	–	33.86	0.47	33.85	0.47
1	33.29	1.72	33.26	1.92	33.89	0.53	33.88	0.54
20	33.54	2.01	33.54	2.01	33.99	0.42	33.99	0.42

margin of the ice (Stat. 158). The significant difference in water column salinities between the ice margin and inner-ice sampling areas was due to much more extensive input of melt water at the Stat. 158. For the same reason, chlorophyll *a* concentrations were also significantly higher at this latter site (cf. Table 2). Surprisingly, a relatively small difference in chlorophyll *a* concentrations was measured between the immediate surface adjacent to melting ice floes and at 20 m depth in the water column. In all cases, the sampling sites were specifically selected immediately adjacent to the brownest patches we could find on ice floe borders. That melting was in progress is clearly indicated by the consistently lower salinity values at the immediate surface in all profiles. A distinctly higher surface chlorophyll *a* concentration, although by only a factor of two, was recorded from only one site (Stat. 156 A).

#### Sea ice algal composition

Pennate diatoms were by far the most abundant organisms in the ice. *Nitzschia cylindrus* was the predominant diatom in all samples. Together with the prymnesiophyte *Phaeocystis* sp., it accounted for more than 80% of the cells in the ice algal community of many of the samples. *N. curta*, *N. prolongatoides*, *N. closterium*, *Tropidoneis belgicae*, *T. van heurckei*, and *Amphiprora* spp. were always present in varying abundances. The remainder of the population comprised other pennate diatoms, low numbers of centric diatoms, many forms of autotrophic and heterotrophic dinoflagellates and small unidentified flagellates, mostly < 8 μm in diameter. Close examination of the ice surface revealed the presence of many small algal aggregates comprised of the above species. These were



**Fig. 2.** Chlorophyll *a* distribution in a survey across the receding ice edge; ice cover > 30% indicated by *dotted area*. *Solid bars* (numbered from 1 to 12) denote sampling sites for which the dominating phytoplankton groups are presented

presumably formed by growth in the confined brine pockets and channels within the ice.

#### Aggregation experiments

Initial chlorophyll *a* and phaeopigment (in parentheses) concentrations in the melted ice samples used for the rotating tank experiments were 61 (2.6), 35 (5.5), and 32 (6.0)  $\mu\text{g l}^{-1}$  from the Stations 169, 180, and 195, respectively. For the same experiments, salinity was 29.8‰, 30.5‰, and 32.3‰, respectively. In the algal assemblages collected from the ice interior (Stats. 169, 180), visible aggregation began immediately after the start of rotation (Fig. 3a, b). Despite the large range of aggregate sizes in the tanks, a rapid increase in size was observed during the first 2 h of rotation. Thereafter, the aggregate size remained more or less constant at an average value of 30–40  $\text{mm}^2$  projected area. For the algal assemblage collected from the infiltration layer of Station 195, no visible aggregation was recorded during the first 7 h (Fig. 3c). During the following

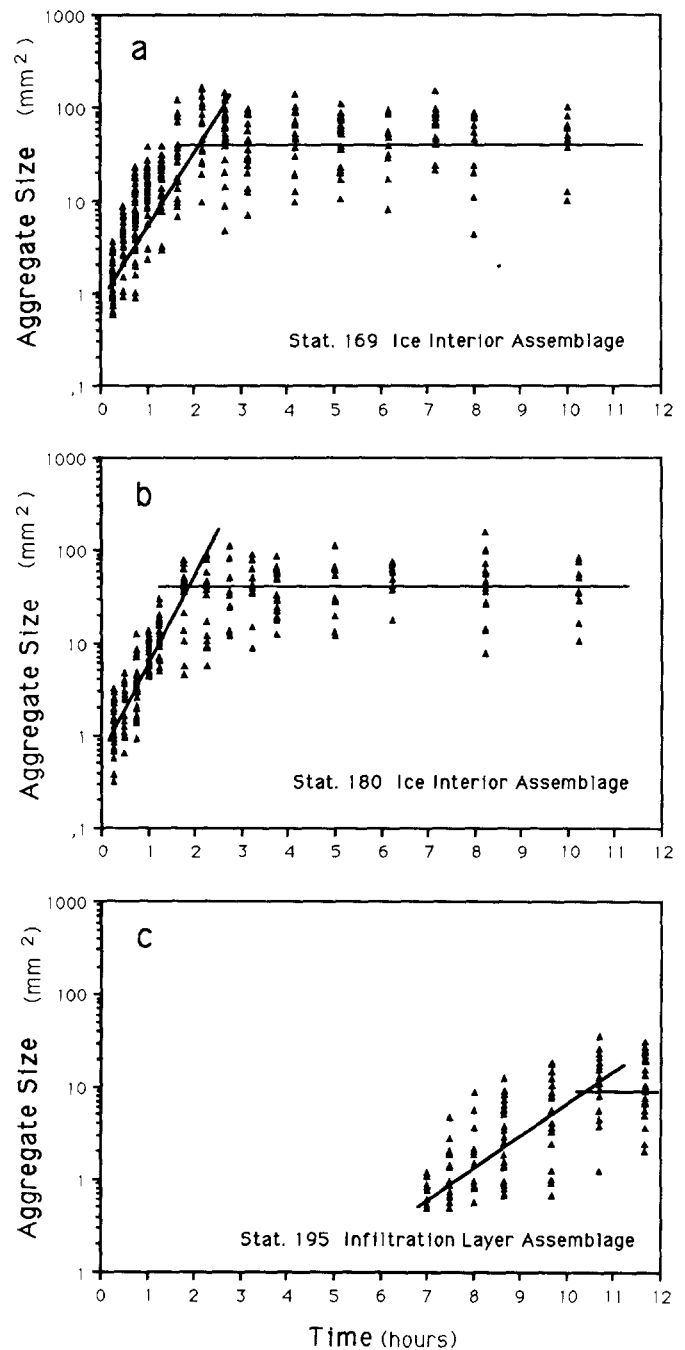


**Fig. 3.** Aggregate size ( $\text{mm}^2$  projected area) in the rotating tanks versus time of rotation; only aggregates > 0.5  $\text{mm}^2$  projected area were recorded. Lines fitted by eye

4 h, small aggregates formed, with sizes slowly increasing to an average of 10  $\text{mm}^2$ .

Microscopic examination of laboratory-made aggregates revealed an algal species composition equivalent to that collected in situ. A comparison of the species composition within aggregates with that of freely suspended algae in the surrounding water showed significant differences (Fig. 4). In subsamples from all experiments, the relative abundance of *Nitzschia cylindrus* and the flagellates in the surrounding water was twice as high as their proportional

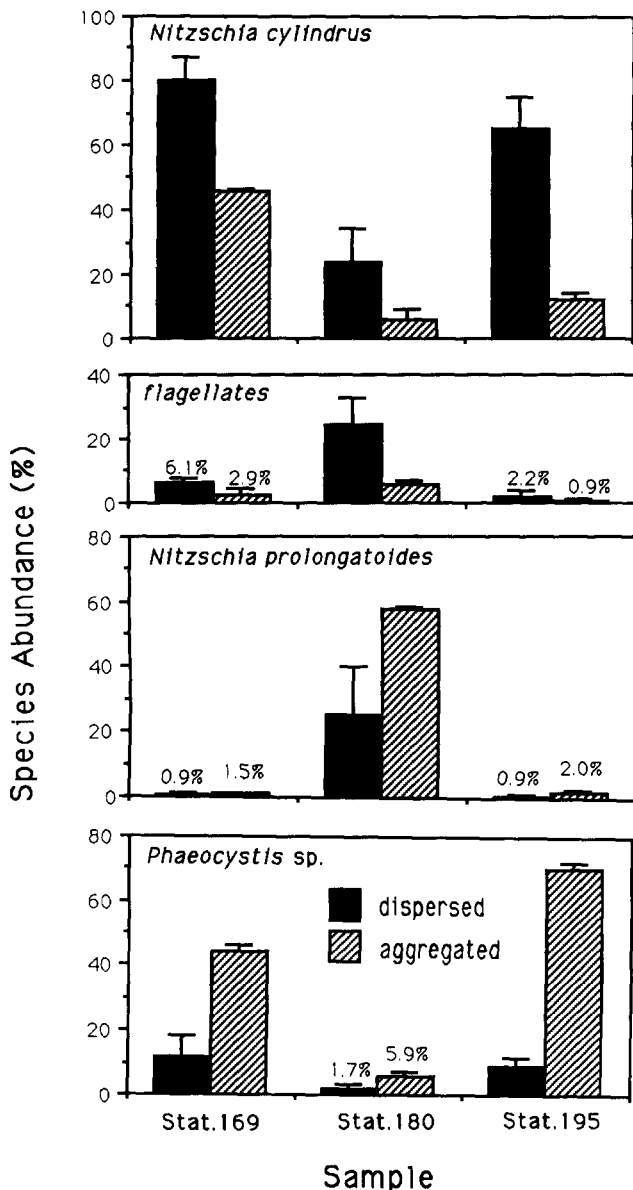


Fig. 4. Relative species abundance of ice algae in aggregates (hatched bars) and dispersed in the surrounding water (solid bars); samples collected from rotating tanks containing melted sea ice samples from Stations 169, 180, and 195

contribution to the aggregates. The opposite was found for *N. prolongatoides* and *Phaeocystis sp.*. The relative abundance of these species in the aggregates always exceeded their occurrence in the surrounding water by a factor of 2 to 3. With some exceptions, a similar relationship was observed for a number of less abundant species, including *Tropidoneis belgicae* and *Amphiprora spp.*

SEM analyses of algal aggregates revealed a distinct structure and a strong patchiness in the distribution of algal species. Macroscopic aggregates formed by the ice interior assemblage of Stats. 169 and 180, ranging between 2 and 10 mm in diameter, were composed of loosely connected subaggregates (approximately 0.5 to 2 mm in

diameter; Fig. 5a). These subaggregates consisted of distinct microaggregates (ca. 100 to 500  $\mu\text{m}$  in diameter), in which ice algal cells, often of monospecific composition, were tightly bound together (Fig. 5b-d). On the other hand, aggregates formed by the infiltration layer assemblage of Stat. 195 revealed a comparatively homogeneous composition and were less clearly structured than aggregates from the ice interior.

Measurements of sinking velocity on a wide range of aggregate sizes revealed a positive relationship between aggregate size and sinking speed (Fig. 6). The sinking rate ranged from 100  $\text{m day}^{-1}$  for the smallest aggregate (ca. 1 mm diameter), to over 500  $\text{m day}^{-1}$  for aggregates with diameters up to 8.5 mm. Aggregates formed by the infiltration layer assemblage of Stat. 195 displayed considerably lower sinking speeds when compared to aggregates of the same size from the ice interior assemblage. Sinking rates of algae that remained dispersed in the surrounding water, as determined by the SETCOL method, were found to be three orders of magnitude smaller than those measured for algal aggregates. Chlorophyll *a*-based sinking rates of cells in the surrounding water averaged 0.36  $\text{m day}^{-1}$  ( $\pm 0.03 \text{ m day}^{-1}$ ) for Stat. 180 and 0.26  $\text{m day}^{-1}$  ( $\pm 0.01 \text{ m day}^{-1}$ ) for Stat. 195.

Distinct differences between aggregated and dispersed algae were also found with respect to metabolic activity (Table 4). At all stations, the rate of oxygen production per unit of chlorophyll *a* for dispersed ice algae was consistently higher by a factor of 1.3 to 2.9 in comparison to algal aggregates. Differences in the rate of respiration in the dark between aggregated and dispersed algae were less pronounced. In general, lower rates were measured for aggregated algae.

## Discussion

Our results show that aggregate formation is a characteristic property of ice algae. The rate at which ice algae released from melting ice formed aggregates in the rotating tanks was exceptionally high when compared with other algae. While in experiments carried out with boreal pelagic diatoms (Riebesell et al., in preparation) initiation of aggregate formation and subsequent growth of aggregate size took place over time periods of days to weeks, rapid aggregation of algae from the ice interior assemblages

Table 4. Oxygen production (light incubation) and respiration (dark incubation) per unit of chlorophyll *a* (in  $\text{ml O}_2 \text{ mg Chl. } a^{-1} \text{ h}^{-1}$ ) of aggregated and dispersed ice algae from sea ice after melting and incubation in rotating tanks, standard deviation in parentheses,  $n=3$

Stat. no.	Light incubation		Dark incubation	
	aggregated	dispersed	aggregated	dispersed
169	1.09 (0.28)	3.16 (0.87)	-0.38 (0.08)	-0.40 (0.12)
180	1.42 (0.46)	1.80 (0.68)	-0.24 (0.03)	-0.26 (0.04)
180	1.10 (0.24)	2.56 (0.32)	-0.32 (0.05)	-0.56 (0.06)
195	2.40 (0.11)	3.37 (0.45)	-0.16 (0.02)	-0.25 (0.04)

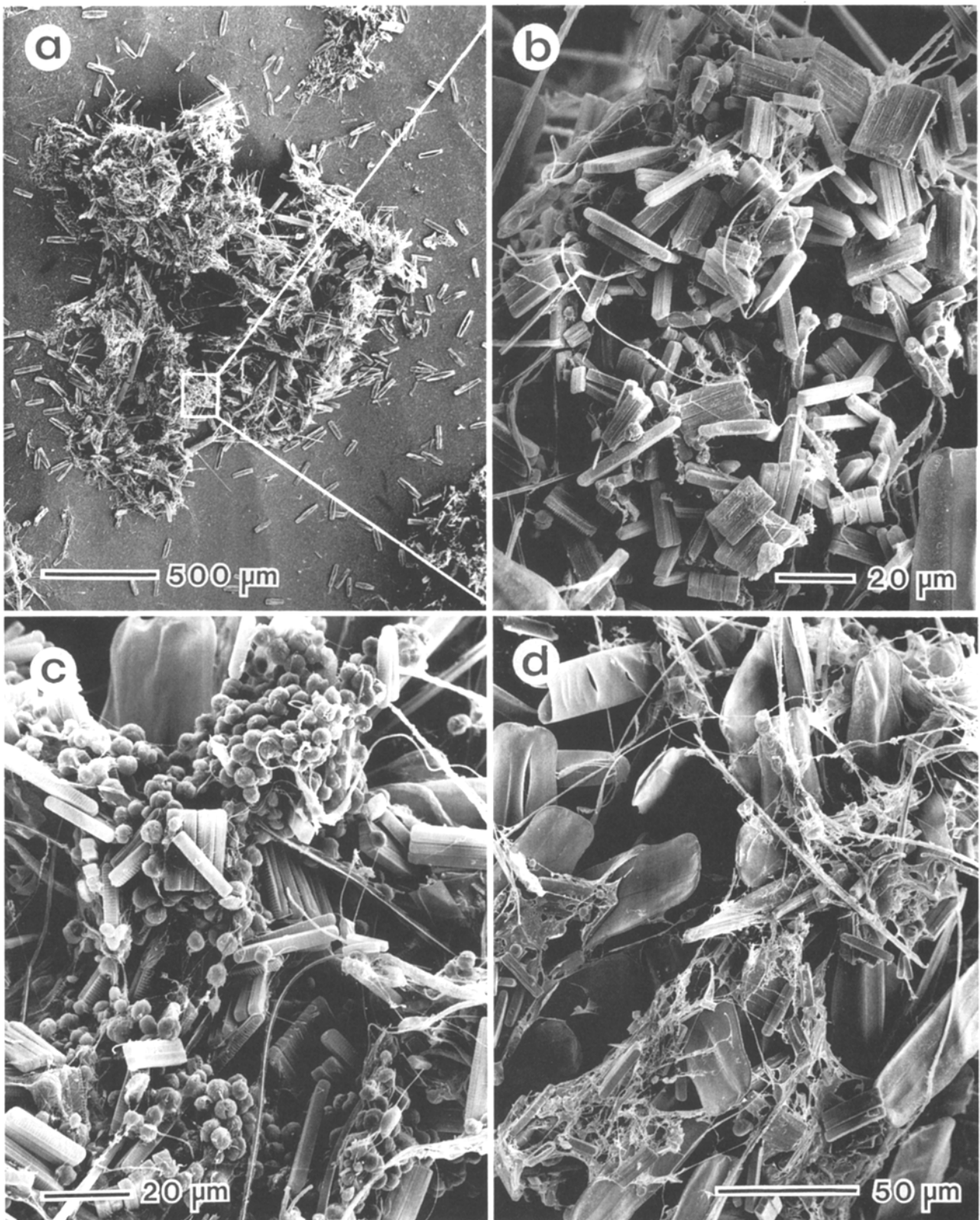


**Fig. 5a–d.** Scanning electron micrographs of aggregates formed by the ice interior assemblage, collected from the rotating tanks; **a** macroaggregate consisting of several subaggregates; **b** enlarged section of the macroaggregate in **a**, monospecific microaggregate of

*Nitzschia cylindrus*; **c** conglomerate of *Phaeocystis* sp. and *N. cylindrus*; **d** microaggregate consisting mainly of *Tropidoneis belgicae* and *N. cylindrus*, partly covered by a wide-meshed mucous web

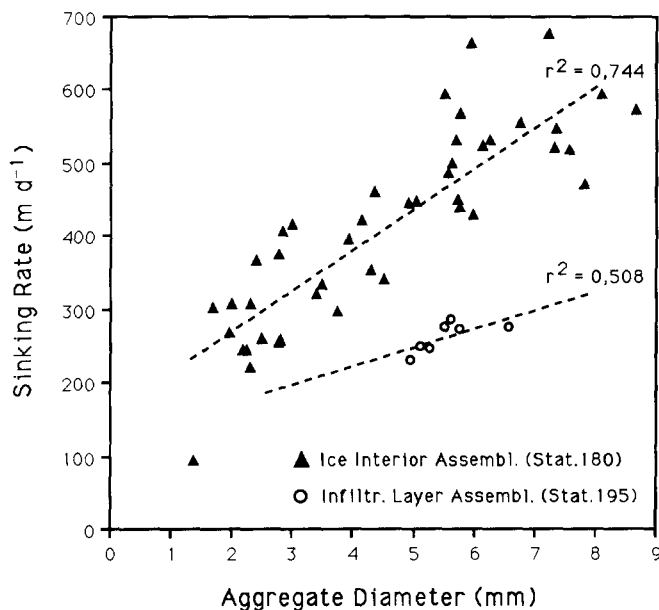


Fig. 6. Sinking rate of ice algal aggregates formed by the ice interior (Stat. 180) and the infiltration layer assemblages (Stat. 195) as a function of aggregate size (mm diameter); aggregates collected from rotating tanks

occurred within the first two hours after release from the melted ice. The unnaturally high concentrations employed for the aggregation experiments with ice algae (chlorophyll *a* concentrations 30–60  $\mu\text{g l}^{-1}$ ), which were chosen to aid observation of aggregate formation, do not invalidate conclusions drawn from these experiments. This assertion is based on extensive experience with cultures of different pelagic diatoms which, after being rotated in the rotating tanks at concentrations above 100  $\mu\text{g Chl. } a \text{ l}^{-1}$  for several days, did not form aggregates. As algal aggregation is primarily determined by the stickiness of the cells, the density of the experimental samples is of secondary importance. Only when cell surfaces have some degree of stickiness will the algal concentration become one of several factors determining the rate of aggregation. In the case of pelagic diatoms, cell stickiness and subsequent aggregation can be induced by a change in the physiological state of the algae such as that caused by nutrient depletion (Kiørboe et al. 1990). From the experiments reported here we conclude that ice algae, in contrast, are inherently sticky.

Many of the dominant ice algae produce extensive extracellular polysaccharide mucilages, which tend to coagulate them into clumps (Bunt and Lee 1969; Cross 1982; McConville and Wetherbee 1983) and permit attachment to the ice substrate (Hoshiai 1977; McConville 1985; Palmisano and Sullivan 1985). In the minute brine pockets of the ice interior, cell division will result in compact accumulations. Cells will not only be attached to the ice substrate but also to each other, thereby initiating formation of the small monospecific microaggregates we observed (Fig. 5b–d). Already within the ice, such microaggregates can clump to larger aggregates (Fig. 5a).

During spring melting, ice algae are released in the form of individual cells, micro-, and macroaggregates. A

strong potential for continuous aggregation of the algae is indicated by the rapid increase in aggregate size in our experiments immediately following release from melted ice (Fig. 3a, b). This implies that the cells and aggregates were not only sticky but were also subject to high encounter rates mediated by differential settling of particles of a wide range of sizes. Given these properties, rapid aggregation will also occur in nature if the released algae are not dispersed. Such conditions could be expected in growing brine channels within melting ice floes and in the shallow melt water lenses accumulating between them (Maykut 1985).

No aggregate formation was recorded during the first 7 h of rotation for the infiltration layer assemblage of Stat. 195 (Fig. 3c). Aggregates forming thereafter were small compared to those from the ice interior assemblage. This difference could be due to the fact that development of the infiltration layer assemblage is a typical spring event and the result of rapid growth within a favourable environment. The metabolism of the infiltration layer algae, and possibly the extent of mucilage secretion, could differ from those inhabiting the ice interior. This is supported by the high rate of oxygen production measured for Stat. 195 in comparison to samples from Stats. 169 and 180 (Table 4). In addition, sinking velocities of aggregates from Stat. 195 were significantly lower than those of equivalently-sized aggregates from Stat. 180 (Fig. 6). It follows that algae from the infiltration layer assemblage would contribute more towards seeding of plankton blooms than those from the ice interior. Mathot et al. (in press) also found much lower photosynthetic efficiencies in assemblages from the ice interior as compared to those from the infiltration layer and the adjacent water column.

The distinct species-specific differences in the degree of incorporation into aggregates (Fig. 4) has ecological implications for the seeding potential of the respective species. Such differences could be induced by the different extents to which various ice algal species secrete mucilage (Allan et al. 1972; McConville 1985). The range of stickiness conferred by differences in composition of the mucilage remains to be examined. Due to the high sinking rates of aggregates (Fig. 6), ice algal cells incorporated into them should rapidly sink out of the euphotic zone in contrast to cells dispersed in the water column. The low relative abundance of *Nitzschia cylindrus* and flagellates in aggregates (Fig. 4) implies that proportionately more cells of these ice algae stay in suspension, thereby increasing their seeding potential. In fact, *N. cylindrus* was found to be the dominating diatom in an ice-edge bloom in the NW Weddell Sea (Garrison et al. 1987) and is considered a typical species of the Weddell Sea summer population (Nöthig 1988). However, this species, although dominant in the ice, was only of minor importance in the water column assemblages during our study.

The recorded differences in the rate of oxygen production and consumption between aggregated and dispersed ice algae (Table 4) suggests that metabolically less active ice algae are concentrated in aggregates, while growing cells are more likely to remain unaggregated. This may imply that inactive cells have a higher tendency to coagulate and, due to high sinking rates of algal aggre-



gates, are more likely to settle out of the euphotic zone. Hence, the process of aggregation could act as a mechanism for selection of cells less adapted to planktonic life. However, the observed difference in photosynthetic oxygen production may also be due to self-shading of algal cells within the aggregates.

Aggregate formation by ice algae will contribute to the vertical flux. Large ice algal aggregates (ranging to more than a cm in diameter) were observed to detach from the undersurface of fast ice and sink to the sea floor (Sasaki and Watanabe 1984; Sasaki and Hoshiai 1986; Carey 1987). Typical ice algae contributed to material collected in traps in the northern Weddell Sea (Gersonde and Wefer 1987). On the other hand, short-term sediment trap deployments in the marginal ice zone during our cruise mainly collected faecal material containing shredded diatom frustules (Cadée and Gonzalez 1989). This would indicate that despite the formation of large aggregates and their potentially high sinking velocities, pelagic grazing is a likely fate of aggregates released from the melting sea ice. Krill (*Euphausia superba*) is known to feed on ice algae by scraping the ice (Marschall 1988). In grazing experiments, krill also fed effectively on suspended ice algal aggregates up to several millimeters in diameter (Riebesell et al. 1989). During both EPOS Leg 1 and 2, numerous krill were observed swimming around ice floes and congregating adjacent to brown patches in melting ice.

As the investigation area is located on the northward flowing flank of the Weddell Gyre, the position of the ice edge is maintained by a steady input of sea ice transported from the southern Weddell Sea. The conditions under which this ice melts will accordingly differ from those prevailing in most of the area seasonally covered by sea ice. In the latter region, the sea ice cover melts simultaneously over extensive areas and not along quasi-stationary ice edges maintained in position over several months. Stabilized melt water layers are more pronounced and algal productivity greater in regions of intensive melting than where melting is extensive. The input of ice algae per unit area is likely to be much larger in regions of intensive melting. Surprisingly, our study shows that the patches of high biomass in melt water lenses were recruited from algal populations that had apparently not flourished in the ice. As the study area is a site of dense krill concentrations that are apparently transported there with the ice (Smetscek et al. 1990), it follows that grazing pressure will also be more intense than in areas of extensive melting. Schalk (1990) found high biomass and substantially higher ETS activity in zooplankton in the ice edge region than further seaward, which supports the idea that grazing pressure will tend to be higher in the marginal ice zone.

A steady release of ice algae in the course of melting could provide a continuous food source for under-ice grazers, whereas a pulsed input of large amounts of ice algal biomass into the water column would lead to rapid sedimentation (Horner 1985). Ackley et al. (1979) concluded that the interior ice assemblage dominating in the Weddell Sea is released over an extended period of time, thus promoting pelagic grazing. However, our observations during this cruise indicate that pulsed input also occurs. On occasion, fields of ice floes were encountered at

the ice edge that were hollowed out horizontally at what had previously been the water level. The intact snow cover was supported, roof-like, over the solid flat base of the ice floe. The ice floes had risen as a result of weight loss and it was possible to discern caverns up to several decimetres high that extended deep into the floe. Such floes were observed following calm, sunny weather. Selective melting of the algal rich layers had evidently occurred due to internal absorption of solar radiation. Under such conditions, ice algae will be pulsed out of the ice prior to large-scale input of melt water and the subsequent formation of a stabilized shallow layer conducive to bloom growth. Such an early, selective input of ice algae will obviate their seeding this shallow layer. On the other hand, ice melting due to heat absorbed by the water could well result in slower melting and enhance the contribution of ice algae to melt water blooms.

In summary, our results indicate that the contribution of typical ice algae to phytoplankton growing in melt water of the Weddell-Scotia Confluence and the northern edge of the Weddell Gyre was not of significance during this investigation. This was demonstrated not only by the large-scale distribution patterns but also by the small-scale survey, as well as measurements immediately adjacent to melting, algal-rich floes. We attribute the negligible seeding effect of ice algae to two factors: a) aggregate formation by the ice algae and their subsequent sinking; b) higher grazing pressure in this region. Apparently, strong regional and possibly temporal differences exist in the contribution of ice algae to water column blooms in the Antarctic.

*Acknowledgements.* We are grateful for the able assistance provided by captain and crew of *RV Polarstern* and appreciated the camaraderie on board. We thank M. Pamatmat for conducting the oxygen measurements and G. Jacques for providing the chlorophyll data presented in Table 2. Thanks also go to N. Vieira for analyzing the photographic material to estimate aggregate size. Critical comments to the manuscript by U. Bathmann, B. Biddanda, M. Botros, G. Diekmann, O. Holm-Hansen, E.-M. Nöthig, and A. Shanks are gratefully acknowledged. Data presented here were collected during the European Polarstern Study (EPOS) sponsored by the European Science Foundation and the Alfred-Wegener-Institute for Polar and Marine Research. Publication number 401 of the Alfred-Wegener-Institute for Polar and Marine Research.

## References

- Ackley SF, Buck KR, Taguchi S (1979) Standing crop of algae in the sea ice of the Weddell Sea region. *Deep-Sea Res* 26A:269–281
- Allan GC, Lewin J, Johnson PG (1972) Marine polymers. IV. Diatom polysaccharides. *Bot Mar* 15:102–108
- Allredge AL, Gotschalk CC (1988) In situ settling behavior of marine snow. *Limnol Oceanogr* 33:339–351
- Allredge AL, Silver MW (1988) Characteristics, dynamics, and significance of marine snow. *Prog Oceanogr* 20:41–82
- Bienfang PK (1981) SETCOL—a technologically simple and reliable method for measuring phytoplankton sinking rates. *Can J Fish Aquat Sci* 38:45–51
- Bunt JS, Lee CC (1969) Observations within and beneath Antarctic sea ice in McMurdo Sound and the Weddell Sea, 1967–1968, Methods and Data, Tech Rep 69-1. Institute of Marine Sciences, University of Miami, Miami

- Cadée G, Gonzalez H (1989) Faeces sedimentation. In: Hempel I, Schalk PH, Smetacek V (eds) The expedition Antarktis VII/3 (EPOS Leg 2) of *RV Polarstern* in 1988/89. Ber Polarforsch 65:165–166
- Carey AG Jr (1987) Particle flux beneath fast ice in the shallow southwestern Beaufort Sea, Arctic Ocean. Mar Ecol Prog Ser 40:247–257
- Cross WE (1982) Under-ice biota at the Pond Inlet ice edge and in adjacent fast ice areas during spring. Arctic 35:13–27
- Daly KL, Macaulay MC (1988) Abundance and distribution of krill in the ice edge zone of the Weddell Sea, austral spring 1983. Deep-Sea Res 35:21–41
- Franeker JA van (1989) Sea ice conditions. In: Hempel I, Schalk PH, Smetacek V (eds) The expedition Antarktis VII/3 (EPOS Leg 2) of *RV Polarstern* in 1988/89. Ber Polarforsch 65:10–13
- Garrison DL, Buck KR (1985) Sea-ice algal communities in the Weddell Sea: species composition in ice and plankton assemblages. In: Gray JS, Christiansen ME (eds) Marine biology of polar regions and effects of stress on marine organisms. John Wiley, New York, pp103–122
- Garrison DL, Buck KR (1986) Organism losses during ice melting: a serious bias in sea ice community studies. Polar Biol 6:237–239
- Garrison DL, Buck KR (1989) The biota of Antarctic pack ice in the Weddell Sea and Antarctic Peninsula regions. Polar Biol 10:211–219
- Garrison DL, Buck KR, Fryxell GA (1987) Sea ice algal communities in Antarctica: species assemblages in pack ice and ice edge planktonic communities. J Phycol 23:564–572
- Gersonde R, Wefer G (1987) Sedimentation of biogenic siliceous particles in Antarctic waters from the Atlantic sector. Mar Micropaleontol 11:311–332
- Hempel I (1989) The expedition Antarktis VII/1 and 2 (EPOS I) of *RV Polarstern* in 1988/89. Ber Polarforsch 62:185
- Hempel I, Schalk PH, Smetacek V (1989) The expedition Antarktis VII/3 (EPOS Leg 2) of *RV Polarstern* in 1988/89. Ber Polarforsch 65:199
- Horner RA (1985) Ecology of sea ice microalgae. In: Horner RA (ed) Sea ice biota. CRC Press, Boca Raton, Florida, pp 83–103
- Hoshiai T (1977) Seasonal change of ice communities in the sea ice near Syowa Station Antarctica. In: Dunbar MJ (ed) Polar oceans. The Antarctic Institute of North America, Calgary, pp 307–317
- Jackson GA (1990) A model of the formation of marine algal flocs by physical coagulation processes. Deep-Sea Res 37:1197–1211
- Kjørboe T, Andersen KP, Dam HG (1990) Coagulation efficiency and aggregate formation in marine phytoplankton. Mar Biol 107:235–245
- Marschall HP (1988) The overwintering strategy of antarctic krill under the pack-ice of the Weddell Sea. Polar Biol 9:129–135
- Mathot S, Becquefort S, Lancelot C (in press) Fate of sea-ice biota at the time of ice melting in the northwestern part of the Weddell Sea. Polar Res
- Maykut GA (1985) The ice environment. In: Horner RA (ed) Sea ice biota. CRC Press, Boca Raton, Florida, pp 21–82
- McConville MJ, Wetherbee R (1983) The bottom-ice microalgal community from annual ice in the inshore waters of East Antarctica. J Phycol 19:431–439
- McConville MJ (1985) Chemical composition and biochemistry of sea ice microalgae. In: Horner RA (ed) Sea ice biota. CRC Press, Boca Raton, Florida, pp 105–129
- Nöthig EM (1988) Untersuchungen zur Ökologie des Phytoplanktons im südöstlichen Weddellmeer im Januar/Februar 1985. Ber Polarforsch 53: 118 pp
- O'Brien DP (1987) Direct observations of the behavior of *Euphausia superba* and *Euphausia crystallorophias* (Crustacea: Euphausiacea) under pack-ice during the antarctic spring of 1985. J Crust Biol 7:437–448
- Palmisano AC, Sullivan CW (1983) Sea ice microbial communities (SIMCO) I. Distribution, abundance, and primary production of ice microalgae in McMurdo Sound, Antarctica in 1980. Polar Biol 2:171–177
- Palmisano AC, Sullivan CW (1985) Growth, metabolism, and dark survival in sea ice microalgae. In: Horner RA (ed) Sea ice biota. CRC Press, Boca Raton, Florida, pp 131–146
- Parsons TR, Maita Y, Lalli CM (1984) A manual of chemical and biological methods for seawater analysis. Pergamon Press, New York, 173 pp
- Riebesell U, Schiel S, Schloss I (1989) Grazing rates in relation to food supply. In: Hempel I, Schalk PH, Smetacek V (eds) The expedition Antarktis VII/3 (EPOS Leg 2) of *RV Polarstern* in 1988/89. Ber Polarforsch 65:160–164
- Sasaki H, Hoshiai T (1986) Sedimentation of microalgae under the Antarctic fast ice in summer. Mem Natl Inst Polar Res, Spec Issue 40:45–55
- Sasaki H, Watanabe K (1984) Underwater observations of ice algae in Lützow-Holm Bay, Antarctica. Antarct Rec 81:1–8
- Schalk PH (1990) Biological activity in the Antarctic zooplankton community. Polar Biol 10:405–411
- Shanks AL, Edmondson EW (1989) Laboratory-made artificial marine snow: a biological model of the real thing. Mar Biol 101:463–470
- Shanks AL, Trent JD (1980) Marine snow: sinking rates and potential role in vertical flux. Deep-Sea Res 27:137–144
- Smetacek V, Scharek R, Nöthig EM (1990) Seasonal and regional variation in the pelagial and its relationship to the life history cycle of krill. In: Kerry KR, Hempel G (eds) Antarctic ecosystems. Springer, Berlin Heidelberg, New York, pp 104–114
- Smith WO, Nelson DM (1985) Phytoplankton bloom produced by a receding ice edge in the Ross Sea: spatial coherence with the density field. Science 227:163–166
- Utermöhl H (1958) Zur Vervollkommnung der quantitativen Phytoplankton-Methodik. Mitt Int Verein Theor Angew Limnol 9:1–38